Published in final edited form as:
J Am Coll Cardiol. 2006 April 18; 47(8): 1707–1712. doi:10.1016/j.jacc.2006.02.040.

Human Degenerative Valve Disease Is Associated With Up-Regulation of Low-Density Lipoprotein Receptor-Related Protein 5 Receptor-Mediated Bone Formation

Frank C. Caira, BSc[*], **Stuart R. Stock, PhD**[†], **Thomas G. Gleason, MD**[*], **Edwin C. McGee, MD**[*], **Jie Huang, ScD**[‡], **Robert O. Bonow, MD, FACC**[*], **Thomas C. Spelsberg, PhD**[§], **Patrick M. McCarthy, MD, FACC**[*], **Shahbudin H. Rahimtoola, MB, FRCP, DSc, MACC, MACP**[‖], and **Nalini M. Rajamannan, MD, FACC**[*]

[*]Division of Cardiology and Cardiothoracic Surgery, Northwestern University Feinberg School of Medicine, Chicago, Illinois

[†]Institute for Bioengineering and Nanoscience in Advanced Medicine, Northwestern University, Chicago, Illinois

[‡]Department of Preventive Medicine, Northwestern University Feinberg School of Medicine, Chicago, Illinois

[§]Department of Molecular Biology and Biochemistry, Mayo Clinic College of Medicine, Rochester, Minnesota

[‖]Division of Cardiovascular Medicine, Department of Medicine, LAC + USC Medical Center, Keck School of Medicine at the University of Southern California, Los Angeles, California

Abstract

OBJECTIVES—The goal of this research was to define the cellular mechanisms involved in myxomatous mitral valve disease and calcific aortic valve disease and to redefine the term degenerative valve disease in terms of an active cellular biology.

BACKGROUND—"Degenerative" valvular heart disease is the primary cause of regurgitant and stenotic valvular lesion in the U.S. However, the signaling pathways are not known. We hypothesize that valve degeneration occurs due to an osteoblastic differentiation process mediated by the low-density lipoprotein receptor-related protein 5 (Lrp5) signaling pathway to cause valve thickening.

METHODS—We examined human diseased valves: myxomatous mitral valves (n = 23), calcified tricuspid aortic valves (n = 27), calcified bicuspid aortic valves (n = 23), and control tissue from mitral and aortic valves (n = 40). The valves were examined by reverse transcriptase-polymerase chain reaction, Western blot, and immunohistochemistry for signaling markers important in osteoblast differentiation: Sox9 and Cbfa1 (transcription factors for osteoblast differentiation); Lrp5 and Wnt3 (osteoblast differentiation signaling marker), osteopontin and osteocalcin (osteoblast endochrondral bone matrix proteins), and proliferating cell nuclear antigen (a marker of cell proliferation). Cartilage development and bone formation was measured by Alcian blue stain and Alizarin red stain. Computed Scano MicroCT-40 (Bassersdorf, Switzerland) analysis measured calcium burden.

Reprint requests and correspondence: Dr. Nalini M. Rajamannan, Northwestern University Feinberg School of Medicine, 300 East Chicago Avenue, Tarry 12-717, Chicago, Illinois 60611. n-rajamannan@northwestern.edu.

RESULTS—Low-density lipoprotein receptor-related protein 5, osteocalcin, and other osteochrondrogenic differentiation markers were increased in the calcified aortic valves by protein and gene expression ($p > 0.001$). Sox9, Lrp5 receptor, and osteocalcin were increased in myxomatous mitral valves by protein and gene expression ($p > 0.001$). MicroCT was positive in the calcified aortic valves and negative in the myxomatous mitral valves.

CONCLUSIONS—The mechanism of valvular heart disease involves an endochondral bone process that is expressed as cartilage in the mitral valves and bone in the aortic valves. Up-regulation of the Lrp5 pathway may play a role in the mechanism for valvular heart disease.

Heart valve “degeneration” is the most common pathologic valve disease in the U.S. and Europe. The spectrum of “degenerative” valve lesions have traditionally been thought to be due to a passive disease process developing rapidly within the valve leaflets. The most common location of these diseased valves is the left side of the heart. Myxomatous mitral valve lesions causing mitral regurgitation are believed to be caused by progressive thickening due to activated myofibroblasts (1). Recent evidence suggests that the aortic valve develops calcification secondary to an osteoblast differentiation pathway (2). Finally, bicuspid aortic valve valves develop calcification similar to that of tricuspid aortic stenosis but at an earlier age (3). The number of surgical valve replacements and surgical valve repairs are increasing in the U.S. due to rapidly aging population.

Despite this increase in prevalence and incidence of valvular heart disease, the signaling pathways in human valve disease have not been identified. Our laboratory and others have recently demonstrated in experimental animal models that bone matrix protein expression in the aortic valve and vasculature are regulated by the low-density lipoprotein receptor-related protein 5 (Lrp5) pathway in the presence of elevated hypercholesterolemia (4,5). The Lrp5, a co-receptor of low-density lipoprotein receptor family, has been discovered as an important receptor in the activation of skeletal bone formation via binding to the secreted glycoprotein Wnt and activating beta-catenin to induce bone formation. Therefore, we hypothesized that the underlying mechanism of “degenerative” valve disease is caused by osteogenic differentiation secondary to the activation of the Lrp5 receptors in human diseased valve leaflets. To test this hypothesis we studied diseased mitral valves, calcified tricuspid, and bicuspid aortic valves to determine if the Lrp5 signaling pathway is expressed in these tissues.

METHODS

Human calcified aortic valves, degenerative mitral valves, and control valves

The use of all human tissue was approved by the human subject protection offices at the Mayo Clinic (1732-98), and Northwestern University (1041-002). Tissues were collected at the time of surgery. We obtained human calcified aortic bicuspid valves (n = 23, mean age 48 years, range 36 to 76 years; men = 13 and women = 10) and tricuspid valves from patients (n = 27, mean age 72 years, range 44 to 93 years; men = 13 and women = 14) at the time of surgical valve replacement. We compared them to degenerative myxomatous mitral valve tissue in patients over the age of 40 years (n = 22, mean age 72 years, range 58 to 85 years; men = 11 and women = 11) removed at the time of surgical valve repair. Normal control valves were obtained from the time of heart transplantation (n = 40, mean age 51 years, range 19 to 56 years; men = 26 and women = 14). Upon dissection, tissues were immersed in formalin for paraffin embedding and frozen at −80°C for ribonucleic acid and protein analysis. Valves were stained for calcification with Alizarin red stain and cartilage with Alcian blue stain.

Immunohistochemistry analysis

Immunohistochemistry for bone matrix markers, cell proliferation, and the Lrp5 pathway was performed as previously described (6). Immunostaining of the valves was performed to identify proliferating cell nuclear antigen (PCNA) (Dako, Carpenteria, California). The following primary antibodies were used for Wnt3/Lrp5 protein expression: anti-Lrp5 (Biovision, Mountain View, California) and anti-Wnt3 (R & D Systems, Minneapolis, Minnesota). Osteopontin, bone sialo-protein and osteocalcin are glycosylated phosphoproteins important in skeletal bone mineralization, and were detected using antibodies obtained from the National Institutes of Health (gift from Dr. Larry Fisher, NIAMS, National Institute of Health) (7,8).

Western blot

Western blot analysis was performed as previously described (4). Anti-Lrp5 (178 Kda) (catalogue number: PAB-10778, Orbigen, San Diego, California), anti-Osteocalcin (58 Kda) (gift from Dr. Larry Fisher, NIAMS, National Institute of Health), beta-catenin (85 Kda) (catalogue number: 2264, Spring Bioscience, Freemont, California), MAPKinase (42 Kda) (anti-p42/44) (catalogue number: 9106, Cell Signaling Technology, Danvers, Massachusetts) were tested to confirm the activation of cellular proliferation; anti-alpha actin (42 Kda) (catalogue number: M0851 Dako) was used as a control. We performed (n = 4) replicates on each Western blot and reverse transcriptase-polymerase chain reaction (RT-PCR) experiment, and show a representative experiment for the data.

Semiquantitative RT-PCR

Immediately after dissection from the heart, the leaflets from each aortic valve were frozen in liquid nitrogen for ribonucleic acid (RNA), extraction. Total RNA was isolated using Trizol reagent (Invitrogen, Carlsbad, California), and 4 μg of RNA were used for semiquantitative RT-PCR analysis. Reverse transcriptase-polymerase chain reaction was performed to determine expression levels of Cbfa1 (289 base pairs [bp]), Sox9 (170 bp), osteocalcin (150 bp), osteopontin (102 bp), cyclin (151 bp), and GAPDH (housekeeping gene) (451 bp) as previously described (2).

MicroCT

After fixing in formalin, the valves were examined using a Scanco MicroCT-40 system (Bassersdorf, Switzerland) operated at 45 kV. Sampling was with ~8 μm voxels (volume elements) and maximum sensitivity (1,000 projections, 2,048 samples, and 0.3 s/projection integration [2]); n = 10 valves total were tested.

Statistics

Data are presented for each diseased valve as an average of the percent of the internal control. The internal control was GAPDH (housekeeping gene) for the polymerase chain reaction and actin for the Western blot. We used one-way analysis of variance to examine if there are differences in normalized gene and protein expression among diseased valves and the control valves, followed by the Dunnett's test to compare the diseased valves to the control valve with adjustment for the multiple comparisons. Significance of the test statistics is set at 0.05 level. Table 1 lists the mean and the standard error for each type of valve tested.

RESULTS

Special stains of the human mitral degenerative valves and calcified aortic valves for bone and cartilage formation

Figure 1 demonstrates the stains for calcification (Alizarin red), cartilage (Alcian blue), and MicroCT. Figure 1A (panels A1 and A2) demonstrates a minimal amount of Alizarin red staining mineralizing tissue present in the control and degenerative mitral valves as compared with the calcified aortic valves, as shown in Figure 1A (panels A3 and A4). In contrast, Figure 1B (panel B2), the Alcian blue cartilage stain, was more intense in the degenerative mitral valves in the areas of the hypertrophic chrondrocyte cells present in the mitral valves (arrow points to hypertrophic chrondrocyte cells). Figure 1B (panel B1) demonstrated a mild amount of cartilage stain in the control valves, and the calcified aortic valves in Figure 1B (panels B3 and B4) demonstrated minimal Alcian blue cartilage stain. Figure 1C (panels C1 and C2) demonstrates that there was no calcification in the control and degenerative mitral valves. The calcified tricuspid and bicuspid aortic valve tissue demonstrated a large amount of calcification as shown in Figure 1C (panels C3 and C4).

Immunohistochemistry of the human mitral degenerative valves and calcified aortic valves for non-collagenous bone matrix synthesis

Figure 2 demonstrates the immunohistochemistry stain for non-collagenous bone matrix proteins: bone sialoprotein, osteopontin, and osteocalcin. There was positive bone sialoprotein staining in the control valves as shown in Figure 2A (panel A1), but this was more intense in the areas of hypertrophic chondrocytes present in the degenerative mitral valves (Fig. 2A, panel A2), as well as the calcified aortic valves as shown in Figure 2A (panels A3 and A4). The osteopontin and osteocalcin stains were more intense in the calcified aortic valves, as shown in Figures 2B (panels B3 and B4) and 2C (panels C3 and C4), as compared with the degenerative mitral valves (Figs. 2B [panel B2] and 2C [panel C2]). The control tissue demonstrated little evidence of osteopontin and osteocalcin (Figs. 2B [panel B1] and 2C [panel C1]).

Immunohistochemistry of the human mitral degenerative valves and calcified aortic valves for endochondral signaling markers Lrp5/Wnt and PCNA

Figure 3 demonstrates the immunohistochemistry stains for the osteoblast signaling markers: Lrp5, Wnt3, and PCNA. Figures 3A (panels A1 and A2) and 3B (panels B1 and B2) demonstrate a mild amount of Lrp5 and Wnt3 staining in the control valves and in the areas of hypertrophic chondrocytes in the mitral valves. The Lrp5 and Wnt3 staining was increased in the calcified aortic valves (Figs. 3A [panels A3 and A4] and 3B [panels B3 and B4]). Figure 3C, panels C3 and C4, demonstrates the presence of an increase in PCNA protein expression as compared with Figure 3C, panels C1 and C2, which demonstrates a decrease in PCNA protein staining.

Western blot, semiquantitative RT-PCR, and MicroCT

Figure 4 demonstrates the Western blot analysis for Lrp5, osteocalcin, beta-catenin (downstream co-transcription factor in the Wnt pathway) and p42/44 (a signaling marker of proliferation) in these valves. Figure 5 demonstrates the semiquantitative RT-PCR for Cbfa1, Sox9, cyclin, osteocalcin, and osteopontin in these valves. Table 1 demonstrates the quantification and statistical analysis of the Western blot and the RT-PCR data. Results from the Dunnett's tests show that using Western blot expression levels in diseased valves are significantly different than those in control valves ($p < 0.001$); using polymerase chain reaction, except for cyclin and osteopontin in bicuspid aortic valve, expression levels in diseased valves are significantly different than those in control valves ($p < 0.001$). One

confounding limitation is the age differences between these diseased valves as we did not age-match these comparison studies.

DISCUSSION

Until recently the etiology of valvular heart disease has been thought to be a “degenerative” process related to the passive accumulation of calcium binding to the surface of the valve leaflet. Recent descriptive studies have demonstrated the critical features of aortic valve calcification, including osteoblast expression, cell proliferation, and atherosclerosis (2,6,9,10), and mitral valve degeneration, glycosaminglycan accumulation, proteoglycan expression, and abnormal collagen expression (11–14). These studies define the biochemical and histologic characterization of these valve lesions.

The most striking phenotypic abnormalities in our study are the formation of cartilaginous structures in the degenerative mitral valves and bone formation in the calcified aortic valves. At the light microscopy level, we were also able to identify hypertrophic chrondrocytes in all of the diseased mitral valves that we studied. We further confirmed a marked increase in Sox9 expression in diseased mitral valves, which is a critical transcription factor in the early stage of cartilage differentiation. In the calcified aortic valves, we found all of the other markers of bone differentiation including the non-collagenous bone matrix proteins osteopontin, osteocalcin, and bone sialoprotein and the osteoblast transcription factor Cbfa1, which were increased in the calcified aortic valves and expressed at a lower level in the degenerative mitral valves.

This study provides protein, gene, and histologic evidence of the spectrum of endochrondral ossification similar to the biology of adult skeleton bone formation. We also tested the hypothesis that valvular osteoblast differentiation occurs in various stages in the mitral valve as compared with the calcified aortic valve, which is regulated by the Lrp5/Wnt3 pathway. We found that the Lrp5/Wnt3 signaling markers are present in the calcified aortic valve greater than the degenerative mitral valve. These data provide the first evidence of a mechanistic pathway for the initiation of bone differentiation in degenerative valve lesions, which is expressed in the mitral valve as a cartilage phenotype and in the calcified aortic valve as a bone phenotype. These results indicate that there is a continuum of an earlier stage of osteoblast bone differentiation in the mitral valves as compared with the calcified aortic valves. The mitral valves did not demonstrate the full osteoblast mineralized phenotype, but an early cartilage phenotype with positive Alcian blue stain and Sox9 expression. In normal adult skeleton formation, the initiation of bone formation occurs with the development of a cartilaginous template, which eventually mineralizes and forms calcified bone. Therefore, the mitral valve expresses an early cartilage formation, and the aortic valve demonstrates the mineralized osteoblast phenotype, which follows the spectrum of normal skeletal bone formation. These data demonstrate the significance of the appearance of thickened mitral valves developing cartilage, which may play a role in the development of severe regurgitation in patients who are older than age 40 years and do not have a clear etiology for the mechanism of mitral valve disease. The calcified aortic valves express an osteoblast phenotype: “bone” in the aortic valve that is responsible for the stenosis present in symptomatic aortic stenosis requiring surgical valve replacement. Our experimental studies further demonstrate that hypercholesterolemia may play a role in the initiating event in these diseases (6,15,16).

This is the first study to demonstrate the presence of chondrocytes in mitral valves, and osteoblasts in aortic valves implicating this pathologic mechanism in the development of mitral regurgitation in myxomatous mitral valves and stenosis in calcific aortic valves. These findings may be secondary to an osteoblast differentiation process that is mediated by

the Lrp5/Wnt3 pathway and demonstrating an active endochondral bone formation mechanism in the development of heart valve disease.

Acknowledgments

The authors would like to thank Janice S. Cruz, MSN, RN, CNP, for her dedication towards recruiting patients for this study.

This work was completed with the support of an American Heart Association Grant-in-Aid (0350564Z) and a grant from the U.S. National Institutes of Health (1K08HL073927-01). Dr. Rajamannan is an inventor on a patent for the mechanisms of valve degeneration. The data in this manuscript is not present in the claims of this patent that was issued in 2003. This patent is owned by the Mayo Clinic, and Dr. Rajamannan does not receive any financial royalties secondary to development of this patent.RT-PCR = reverse transcriptase-polymerase chain reation.

Abbreviations and Acronyms

Lrp5	low-density lipoprotein receptor-related protein 5
PCNA	proliferating cell nuclear antigen
RNA	ribonucleic acid
RT-PCR	reverse transcriptase-polymerase chain reaction

REFERENCES

1. Rabkin E, Aikawa M, Stone JR, et al. Activated interstitial myofibroblasts express catabolic enzymes and mediate matrix remodeling in myxomatous heart valves. Circulation. 2001; 104:2525–2532. [PubMed: 11714645]
2. Rajamannan NM, Subramaniam M, Rickard D, et al. Human aortic valve calcification is associated with an osteoblast phenotype. Circulation. 2003; 107:2181–2184. [PubMed: 12719282]
3. Roberts WC, Ko JM. Frequency by decades of unicuspid, bicuspid, and tricuspid aortic valves in adults having isolated aortic valve replacement for aortic stenosis, with or without associated aortic regurgitation. Circulation. 2005; 111:920–925. [PubMed: 15710758]
4. Rajamannan NM, Subramaniam M, Caira F, et al. Atorvastatin inhibits hypercholesterolemia-induced calcification in the aortic valves via the Lrp5 receptor pathway. Circulation. 2005; 112(Suppl 9):I229–I234. [PubMed: 16159822]
5. Shao JS, Cheng SL, Pingsternhaus JM, et al. Msx2 promotes cardiovascular calcification by activating paracrine Wnt signals. J Clin Invest. 2005; 115:1210–1220. [PubMed: 15841209]
6. Rajamannan NM, Subramaniam M, Springett M, et al. Atorvastatin inhibits hypercholesterolemia-induced cellular proliferation and bone matrix production in the rabbit aortic valve. Circulation. 2002; 105:2260–2265.
7. Kerr JM, Fisher LW, Termine JD, et al. The cDNA cloning and RNA distribution of bovine osteopontin. Gene. 1991; 108:237–243. [PubMed: 1721033]
8. Kerr JM, Fisher LW, Termine JD, et al. The human bone sialoprotein gene (IBSP): genomic localization and characterization. Genomics. 1993; 17:408–415. [PubMed: 8406493]
9. O'Brien KD, Kuusisto J, Reichenbach DD, et al. Osteopontin is expressed in human aortic valvular lesions (comment). Circulation. 1995; 92:2163–2168. [PubMed: 7554197]
10. Mohler ER 3rd, Gannon F, Reynolds C, et al. Bone formation and inflammation in cardiac valves. Circulation. 2001; 103:1522–1528. [PubMed: 11257079]
11. Whittaker P, Boughner DR, Perkins DG, et al. Quantitative structural analysis of collagen in chordae tendineae and its relation to floppy mitral valves and proteoglycan infiltration. Br Heart J. 1987; 57:264–269. [PubMed: 3566985]
12. Wooley CF, Baker PB, Kolibash AJ, et al. The floppy, myxomatous mitral valve, mitral valve prolapse, and mitral regurgitation. Prog Cardiovasc Dis. 1991; 33:397–433. [PubMed: 2028020]

13. Grande-Allen KJ, Borowski AG, Troughton RW, et al. Apparently normal mitral valves in patients with heart failure demonstrate bio-chemical and structural derangements: an extracellular matrix and echocardiographic study. J Am Coll Cardiol. 2005; 45:54–61. [PubMed: 15629373]

14. Grande-Allen KJ, Calabro A, Gupta V, et al. Glycosaminoglycans and proteoglycans in normal mitral valve leaflets and chordae: association with regions of tensile and compressive loading. Glycobiology. 2004; 14:621–633. [PubMed: 15044391]

15. Makkena B, Salti H, Subramaniam M, et al. Atorvastatin decreases cellular proliferation and bone matrix expression in the hypercholesterolemic mitral valve. J Am Coll Cardiol. 2005; 45:631–633. [PubMed: 15708716]

16. Rajamannan NM, Subramaniam M, Stock SR, et al. Atorvastatin inhibits calcification and enhances nitric oxide synthase production in the hypercholesterolaemic aortic valve. Heart. 2005; 91:806–810. [PubMed: 15894785]

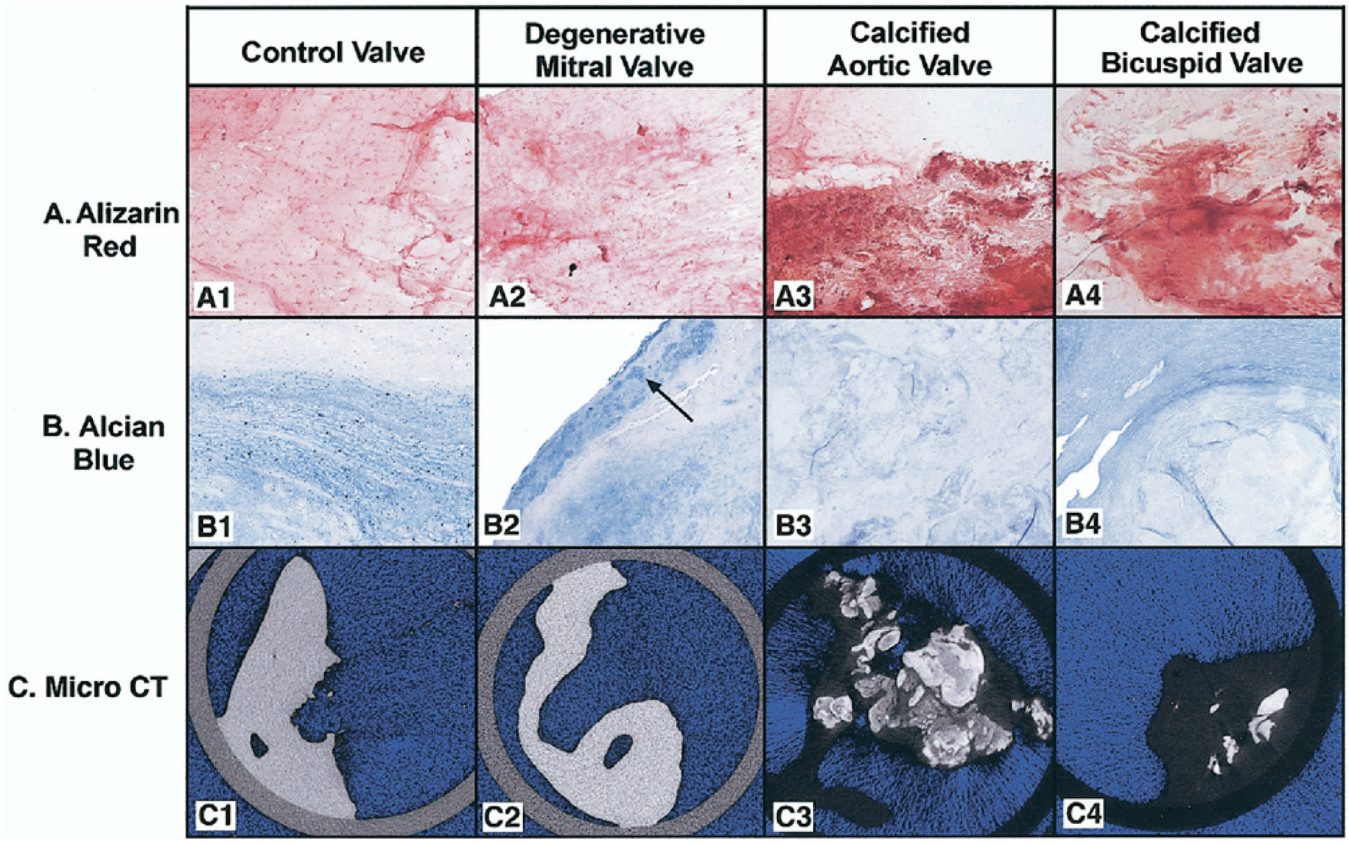

Figure 1.

Immunohistochemistry of the human mitral degenerative valves and calcified tricuspid and bicuspid aortic valves for calcification, cartilage, and MicroCT scan. Control valve, degenerative mitral valve (**arrow** points to hypertrophic chondrocytes), calcified aortic valves (**arrow** points to positive stain), and bicuspid aortic valve (arrow points to positive stain) (magnification 25×). (**A**) Alizarin red stain. (**B**) Alcian blue stain. (**C**) MicroCT scan (**gray area** is the soft tissue, **white** area is calcification, **blue** is the background).

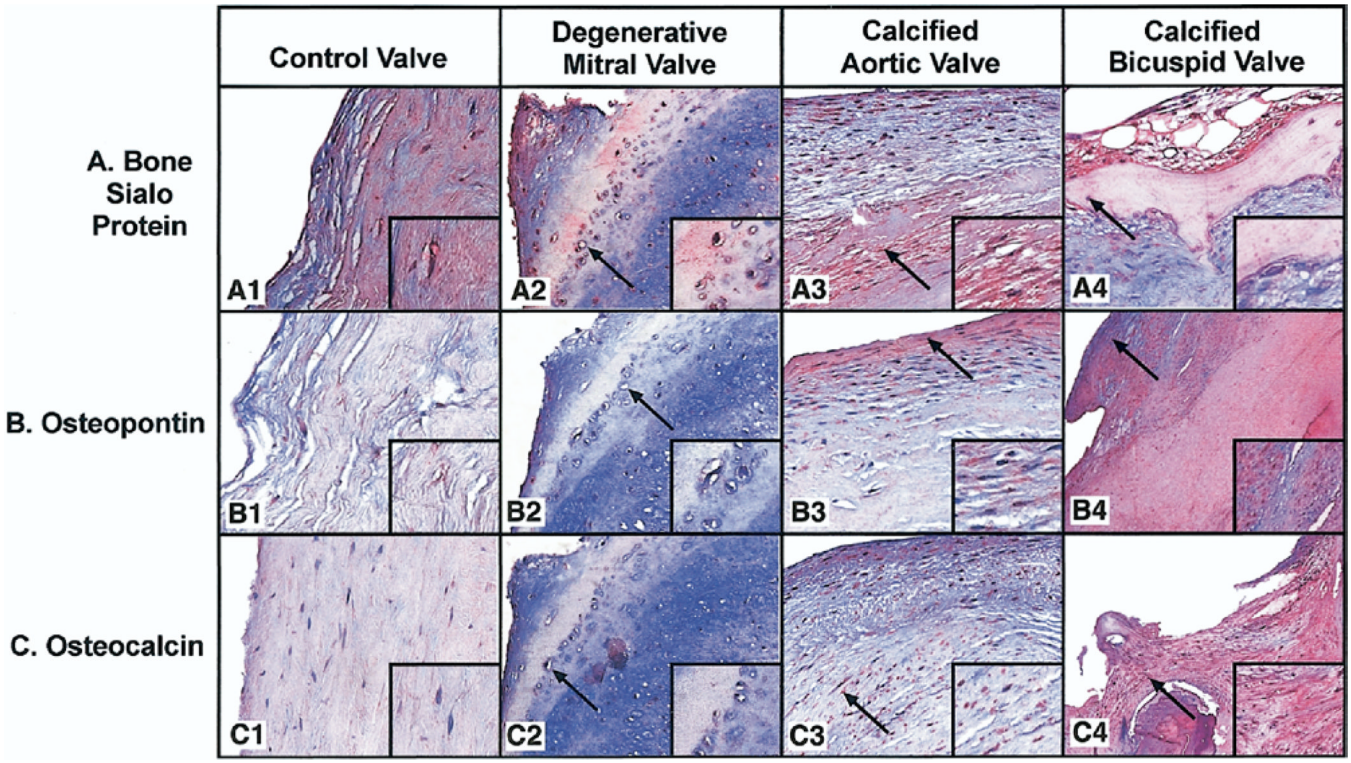

Figure 2.

Immunohistochemistry of the human mitral degenerative valves and calcified tricuspid and bicuspid aortic valves for non-collagenous bone matrix synthesis. Control valve, degenerative mitral valve (**arrow** points to hypertrophic chondrocytes), calcified aortic valves (**arrow** points to positive stain), and bicuspid aortic valve (arrow points to positive stain) (magnification 25×). **Insert** within each photo is a high-power magnification to demonstrate cellular staining (magnification 40×). (**A**) Bone sialoprotein stain. (**B**) Osteopontin stain. (**C**) Osteocalcin stain.

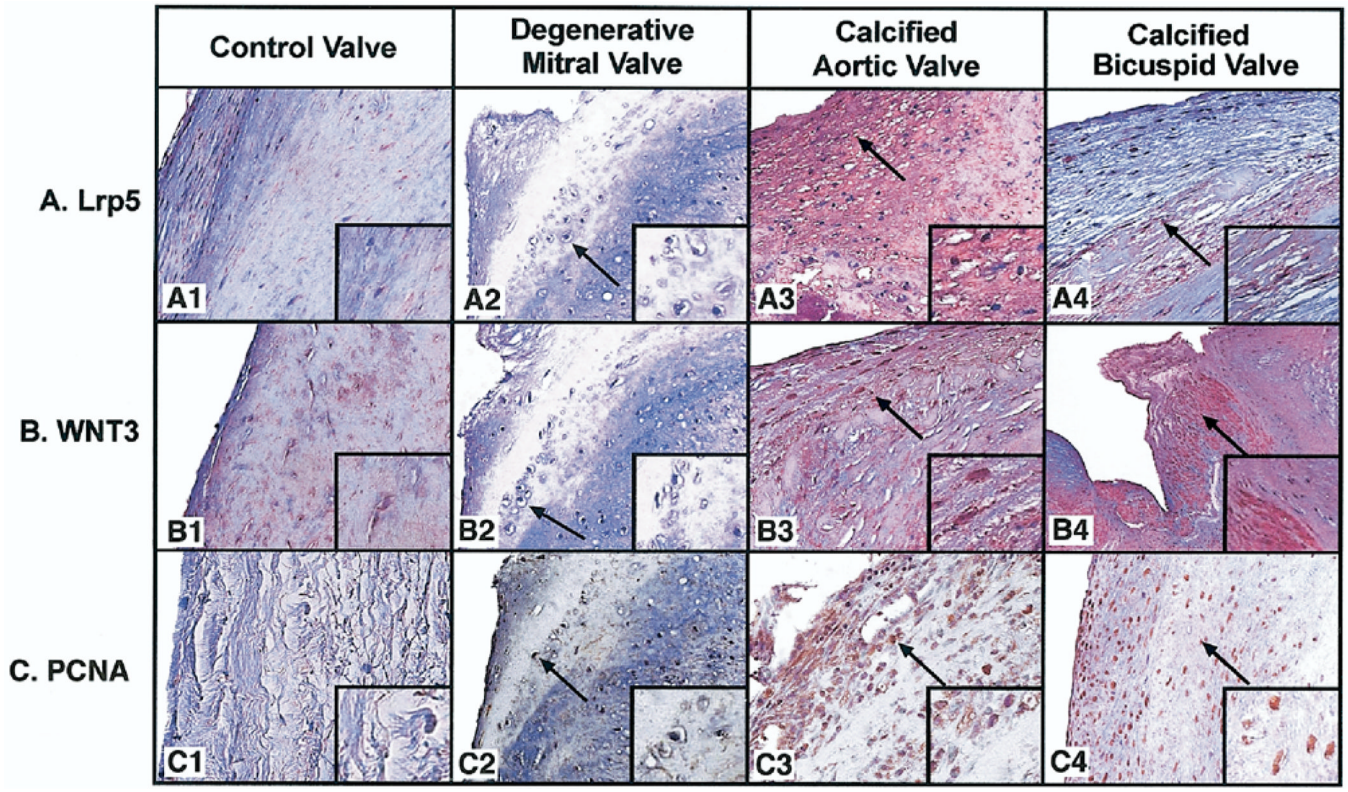

Figure 3.

Immunohistochemistry of the human mitral degenerative valves and calcified tricuspid and bicuspid aortic valves for endochondral signaling markers low-density lipoprotein receptor-related protein 5/Wnt and proliferating cell nuclear antigen. Control valve, degenerative mitral valve (**arrow** points to hypertrophic chondrocytes), calcified aortic valves (**arrow** points to positive stain), and bicuspid aortic valve (**arrow** points to positive stain) (magnification 25×). **Insert** within each photo is a high-power magnification to demonstrate cellular staining (magnification 40×). (**A**) lipoprotein receptor-related protein 5 stain. (**B**) Wnt 3 stain. (**C**) Proliferating cell nuclear antigen stain.

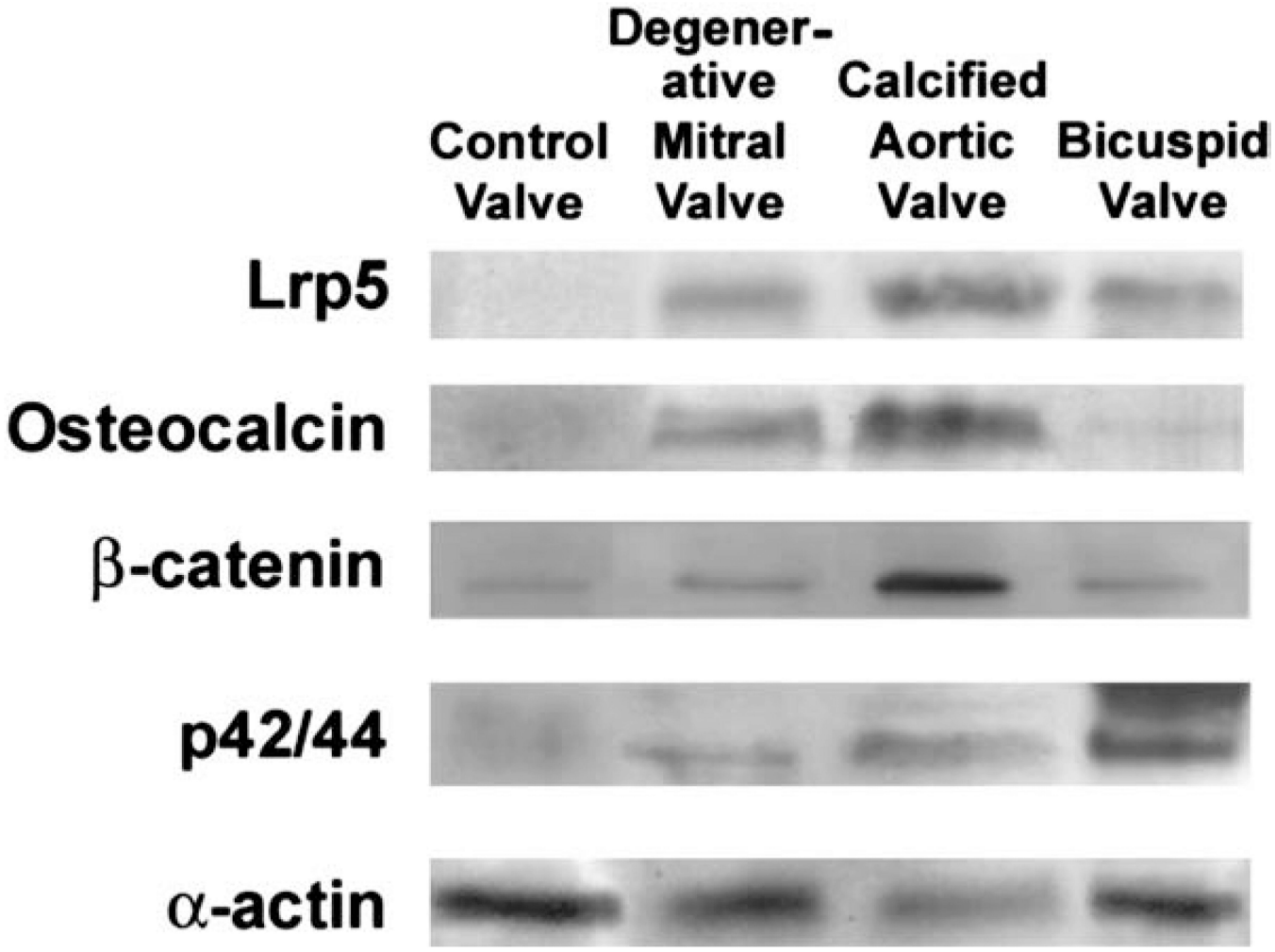

Figure 4.
Western blot. Western blot analysis for lipoprotein receptor-related protein 5 (Lrp5), osteocalcin, β-catenin, p42/44, and α-actin.

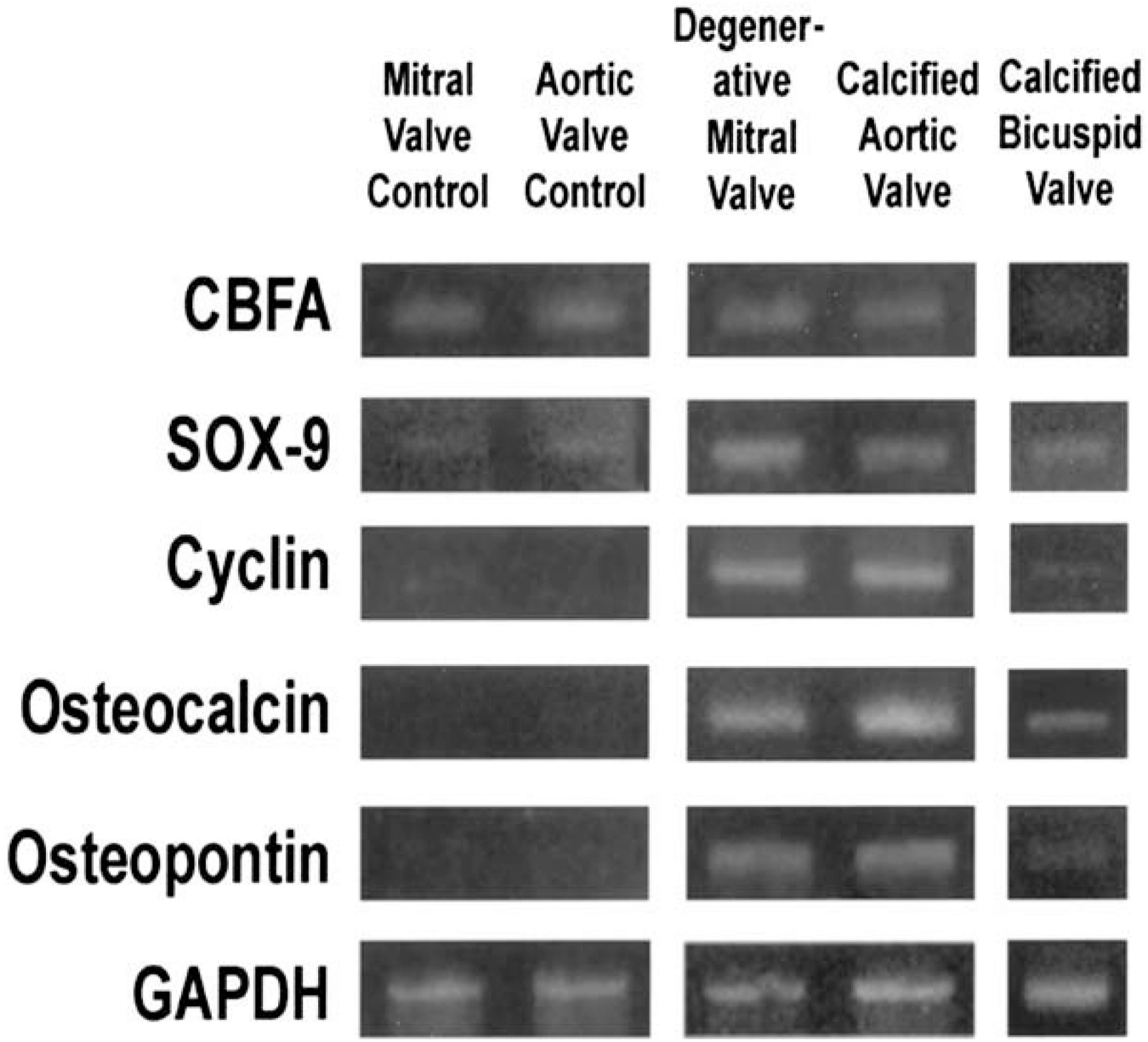

Figure 5.
Semiquantitative reverse transcriptase-polymerase chain reaction. Reverse transcriptase-polymerase chain reaction results for Cbfa1, Sox9, cyclin, osteocalcin, and osteopontin.

Table 1

Quantitative Analysis of Western Blot and RT-PCR

	Control Valve	Degenerative Mitral Valve	Calcified Aortic Valve	Calcified Bicuspid Valve
Western				
Lrp5	0.27 ± 0.01	0.58 ± 0.01*	0.94 ± 0.01*	0.60 ± 0.01*
Osteocalcin	0.60 ± 0.01	0.56 ± 0.00†	1.20 ± 0.01*	0.69 ± 0.01*
Beta-catenin	0.58 ± 0.01	0.68 ± 0.01*	2.29 ± 0.01*	0.70 ± 0.01*
p42/44	0.62 ± 0.01	0.57 ± 0.01†	0.86 ± 0.01*	1.02 ± 0.01*
RT-PCR				
Cbfa 1	0.64 ± 0.01	0.82 ± 0.00*	0.82 ± 0.01*	0.43 ± 0.01†
SOX 9	0.57 ± 0.01	1.02 ± 0.03*	0.80 ± 0.01*	0.85 ± 0.02*
Cyclin	0.59 ± 0.01	1.09 ± 0.01*	1.15 ± 0.02*	0.54 ± 0.01
Osteocalcin	0.39 ± 0.01	1.14 ± 0.04*	1.21 ± 0.03*	0.76 ± 0.01*
Osteopontin	0.45 ± 0.01	1.10 ± 0.02*	0.85 ± 0.01*	0.49 ± 0.01

*Value increase greater than control, $p \leq 0.001$.

†Value decrease less than control, $p < 0.001$.

RT-PCR = reverse transcriptase-polymerase chain reaction.